# Covariant *ab initio* Approach to Nuclear Matter, Nuclei and Neutron Stars

Horst Lenske, Urnaa Badarch, Patrick Konrad, Sonja Orrigo, and Nadia Tsoneva
Institut für Theoretische Physik,
Universität Giessen, D-35392 Giessen, Germany

**Abstract**

Nuclear matter and finite nuclei at extreme isospin are studied the DDRH field theory. In-medium interactions in nuclear and hypernuclear matter are described with density dependent meson-baryon vertex functionals, derived from Dirac-Brueckner theory. Relativistic mean-field results are presented ranging from nuclear matter over isotopic chains of nuclei to neutron stars. Dynamical correlations from pairing interactions and core polarization are found to increase strongly when approaching the driplines. Above particle threshold core polarization gives rise to narrow *Fano Resonances* as new mode of continuum excitation. This is accompanied by a strong reduction of mean-field configurations, as indeed observed in recent experiments. Anharmonicities in dipole excitations are investigated along isotopic chains including up to three phonon admixtures and using microscopic HFB quasiparticle input. Pygmy dipole resonances are found to provide a clear signature for neutron skins.

## 1 Introduction

Our knowledge about the mass and charge dependence of nuclei can be cast into a formula as simple as the well known Bethe-Weiszäcker Mass Formula [1], describing the binding energies of the about 2500 known nuclides with about 8 parameters. This remarkable simplicity is still a puzzling result, when considered from the side of nuclear many-body theory. This is true, independently whether traditional non-relativistic models or more modern field theoretical or QCD-inspired theories are used. To understand how the competition among the various nuclear degrees of freedom leads from complexity to simplicity is the major challenge of nuclear theory. The new experimental developments in the recent past [2, 3, 4] and the promising plans for new facilities, among which FAIR [6] will play a central role, are giving us access to new regions of the nuclear chart, thus allowing to explore nuclear dynamics under extreme conditions of large charge asymmetry and weak binding.

Experiments with rare isotopes indicate significant deviations from the dynamics of stable nuclei. Under such conditions the conventional binding mechanisms of $\beta$ stable nuclei are likely to change. As a consequence, the quasi-particle picture and the closely related mean-field concept cannot be expected to remain the major building blocks of nuclear dynamics but will be in competition with dynamical correlations among a few nucleons or clusters of nucleons.

These modifications are due to the strong enhancement of isovector interactions with increasing neutron or proton excess [5]. In beta-stable nuclei one is used to have minor to negligible isovector effects because in the valley of stability charge asymmetry is constrained to proton-to-mass ratios around $\xi = Z/A \simeq 0.5$ and the strength of the isovector mean-field behaves as $\sim 1 - 2\xi \sim 0$. In an extremely neutron-rich nucleus, however, asymmetries down to $\xi \sim 0.25$ are found, e.g. in the neutron-rich $He$ and $Li$ isotopes. Under such conditions the isovector potential is strongly enhanced to values which are comparable to the overall attractive isoscalar potential. As a result, in a neutron-rich nucleus the neutrons are moving in a rather shallow potential with a depth of only 1/3 of the proton potential. As a consequence the single particle spectrum is considerably compressed, observed as reduced shell or sub-shell spacings or even inversions in the ordering of levels. The most dramatic effect is found in the valence shells. They are pushed close to the continuum threshold with separation energies $\ll 1$ MeV, one or two orders of magnitude less than in well bound stable nuclei. In extreme cases where the mean-field ceases to bind the outermost nucleons, self-energies from collisional processes, i.e. dynamical core polarization, will take over. Such dynamical self-energies produce bound states of a new kind, not being related to the mean-field. For such systems a description in terms of the traditional mean-field concepts is inadequate and may even result in confusing and contradictory conclusions.

In this contribution we will elaborate on the new type of dynamics encountered far off stability. In sect. 2 nucleon-nucleon ($NN$) interactions in symmetric and asymmetric nuclear matter will be discussed. Dirac-Brueckner theory is used to derive in-medium interaction [7] from well established free-space NN meson exchange

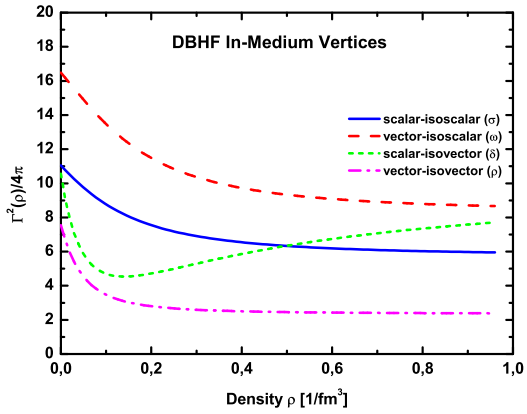


Figure 1: Density dependence of the in-medium meson-nucleon vertices. Results for the sigma (full), delta (long dashed), omega (short dashed), and rho (dashed-dotted) interaction channels obtained from DBHF calculations with the Groningen NN-potential are shown up to neutron star densities [7, 9, 17].

potentials. By means of the Density Dependent Relativistic Hadron ($DDRH$) field theory [8, 9, 17] density dependent meson-nucleon vertex functionals are determined which, in turn, are applied in sect. 3 in calculations for infinite nuclear matter, neutron stars and ground states of finite nuclei [9, 17, 18] and hypernuclei [19, 20].

Non-relativistic many-body theory is the background for the topics to be discussed in the remaining sections. In sect. 4 dynamical self-energies from short range correlations and core polarization are investigated and we introduce Fano-resonances as a new mode in exotic nuclei. Nuclei with a neutron skin are considered in sect. 5. Low energy electric dipole strength is studied over the $Sn$ isotopic chain in a microscopic QRPA multi-phonon model [11, 12, 13]. The so-called Pygmy Dipole Resonance ($PDR$) mode is found to be a clear signature of a neutron skin. In sect. 6 the various topics are summarized, conclusions are drawn and an outlook is given.

## 2 Interactions in Asymmetric Nuclear Matter

We describe interactions among nucleons and hyperons in a common field theoretical boson exchange approach [9]. The NN interactions include isoscalar and isovector pseudoscalar ($\eta$, $\pi$), scalar ($\sigma$, $\delta/a_0(980)$) and vector ($\omega$, $\rho$) mesons. Extensions into the strangeness sector are accomplished by taking into account also the strangeness-carrying members of the pseudoscalar, vector and scalar meson octets. The scalar octet, to which the $\sigma$ and the $\delta$ mesons would belong, is empirically not well established but is essential for understanding baryonic interactions.

We describe free space and in-medium interactions in a Lagrangian formulation

$$\mathcal{L} = \mathcal{L}_B + \mathcal{L}_M + \mathcal{L}_{BM} \tag{1}$$

where $\mathcal{L}_B$ and $\mathcal{L}_M$ are the Lagrangians of non-interacting baryons and mesons. Their interactions are contained in

$$\mathcal{L}_{BM} \sim g\overline{\Psi}_B\Gamma_\alpha\Psi_B\Phi_M^\alpha \tag{2}$$

including a (set of) coupling constant(s) $g$ and otherwise are given by Lorentz-invariant combinations of the baryon $\Psi_B$ and meson field $\Phi_M$ operators including appropriate Dirac vertices $\Gamma$, see e.g. [8].

Such a Lagrangian model is known, e.g. [7, 9, 10], to lead to baryon-baryon ($BB$) meson-exchange potentials of the form

$$V_{mBB'}(q',q) = \frac{g^2_{mBB'}}{4\pi}\overline{\psi}_B(q)\Gamma_\alpha\psi_{B'}(q')^\dagger D_m(q-q')\overline{\psi}_B(q)\Gamma^\alpha\psi_{B'}(q') \tag{3}$$

where $D_m(q-q')$ is the momentum space Klein-Gordon propagator for meson $m$. Since we have to deal with the coupling constants $\mathcal{O}(g) > 1$ the full perturbation series has to be summed. In the present context this

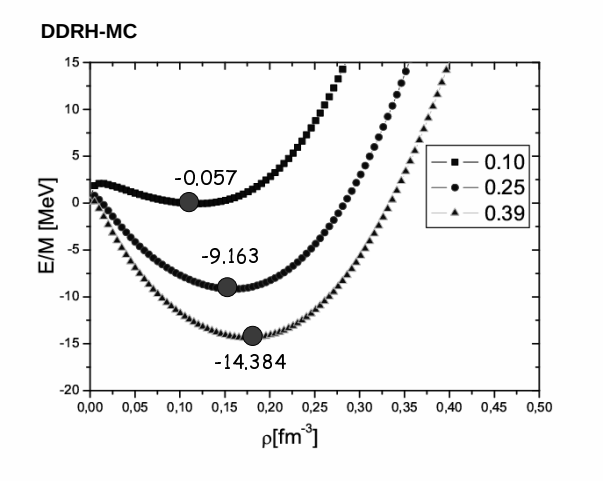


Figure 2: The DDRH nuclear equation of state for three different asymmetries (see text).

means to solve the Bethe-Salpeter equation [16]

$$T(q', q|\sqrt{s}, k_F) = V(q', q) + \int \frac{d^3k}{(2\pi)^3} V(q', k) g_{NN}(k|\sqrt{s}, k_F) Q_F(k|\sqrt{s}, k_F) T(k, q|\sqrt{s}, k_F) \quad , \tag{4}$$

including the usual reduction to three space-like dimensions [9, 10, 9].

The medium affects the solutions of eq. 4 in the first place via the Pauli-projector $Q_F$ by which the occupied regions inside the Fermi-sphere $k \leq k_F$ are excluded from the intermediate two-particle states. Higher order corrections are provided by the modifications of the propagators and vertices due to self-energies [9]. Eq. 4 has to be solved at total center of mass energy $\sqrt{s}$, the relative momenta $q, q'$ and given Fermi-momentum $k_F$.

A better insight into the structure and properties of in-medium interactions is gained by representing the scattering amplitudes $T(q', q|\sqrt{s}k_F)$ again in a basis of meson exchange potentials [7, 8, 9, 19]. Hence, we represent the half off-shell T-matrix

$$T(q, q_s|\sqrt{s}, k_F) = \sum_m z_m(\sqrt{s}, k_F) V_m(q, q_s) \tag{5}$$

in terms of (elementary) meson exchange potentials $V_m$, eq. 3, and *density dependent* vertex renormalization factors $z_m(\sqrt{s}, k_F) > 0$. Above, $q' = q_s$ denotes the on-shell momentum related to the Mandelstam variable $s$. Note that at vanishing density $k_F \to 0$ $z_m(\sqrt{s}, k_F) \to \zeta_m(\sqrt{s})$ is approached where in general $\zeta_m(\sqrt{s}) \neq 1$ because then eq.5 provides a re-parametrization of the full NN scattering amplitude in free space. After averaging over the dependence on $\sqrt{s}$ the above *ansatz* leads to the density dependent in-medium meson-nucleon vertices [7]

$$\Gamma_m(k_F) = z_m(k_F) g_m \sim g_m \left(1 - h_m(k_F^2) g_m^2 + \mathcal{O}(g_m^4)\right) \quad , \tag{6}$$

where $h_m(k_F^2)$ is directly related to the underlying Bethe-Salpeter equation [9].

DBHF results for $\Gamma_m(\rho)$ in the mean-field relevant interaction channels are displayed in Fig.1 over a density range up to neutron star densities. With the exception of the scalar-isovector channel the vertices decrease with increasing density. In all cases, including also the $\delta/a_0$ channel, a plateau seems to be approached at high density resembling a saturation behavior. In Fig.2 the nuclear equation of state for asymmetries ranging from Pb ($\xi = Z/A = 0.39$) to the limit of binding ($\xi = 0.1$) are displayed. With increasing asymmetry the saturation point is seen to move steadily to lower densities and the binding energy diminishes.

## 3 Density Dependent Field Theory

Once we have obtained the density dependent vertices in infinite nuclear matter the question arises how to apply them in a meaningful way to finite nuclei and other systems of interest, e.g. to neutron stars and extensions to hypernuclei allowing to study the full SU(3) flavor sector. This is achieved by the formulation of a field theory with vertex functionals depending on the field operators. We use a Lagrangian of the same basic structure as in eq.1 and eq.2 [9, 17] but now the meson-baryon interactions are described by vertex functionals $g^*(\varphi_i)$

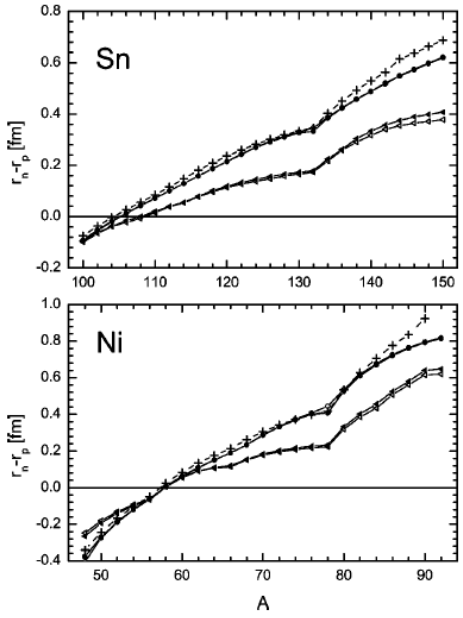


Figure 3: Thickness of the neutron skins in the Sn and Ni isotopes. DDRH results [9, 17] are for the Bonn A ($a_4 = 32$ MeV) and the Groningen NN ($a_4 = 26$ MeV) potential are displayed.

depending in a Lorentz-invariant manner on the field operators $\varphi_i$ of the underlying hadronic field theory [9]. Hence, the vertices have gained an intrinsic dynamical structure on their own. The quantum character of the system is retained if the functional structure of the vertices is expressed in terms of the baryon field operators $\Psi_B$ [8, 9].

As shown in a series of papers [8, 9, 17, 18, 19, 20] on the Density Dependent Relativistic Hadron (DDRH) field theory this requires special care on how to treat the non-linearities such that a covariant and thermodynamically consistent theory is obtained. The functional structure of the vertices leads to additional baryonic rearrangement self-energies which are indispensable for thermodynamical consistency as was proven in [8]. The DDRH theory provides a general frame work for such studies. In fact, being theoretically much more safely founded than the conventional relativistic mean-field approach [14] the DDRH formulation is being used by other groups, e.g. [24, 25, 26, 27] on an empirical level. The most significant advantage is that a parameter-free description of nuclear many-body systems is achieved once DDRH and DBHF theory are combined. As discussed in the cited papers choosing a free-space NN meson exchange potential and performing a DBHF calculation in infinite matter fixes completely the interactions at all densities. The DDRH predictions are easily tested in calculations for finite nuclei. Typical results are presented in Fig.3 where total binding energies for Ni isotopes are compared to data. Indeed, without any special adjustment of parameters the DDRH results agree convincingly well with the measured values thus confirming the approach. The DDRH calculations show that with increasing neutron excess medium and heavy nuclei like the Ni and Sn isotopes, respectively, develop an increasingly pronounced neutron skin [11, 12, 13, 17] which at the extreme can exceed the extension of the bulk by more than 0.5 fm.

The DDRH approach has been extended into the strangeness sector in [19, 20] by considering infinite hyper matter and single $\Lambda$ hypernuclei. Using meson-hyperon vertices obtained in a semi-microscopic approach the available $\Lambda$ hypernuclear data are well described. Auger neutron spectra from ejecting a neutron after electroproduction and capture of a $\Lambda$ were investigated in [20] as a spectroscopic tool for hypernuclei. A corresponding experiment is in preparation at JLAB. In a naive quark model one would expect that the $\Lambda$ vertices are reduced to 2/3 of the nucleonic values. However, this is only true on the tree level because resummation as in eq.4 will alter the relations. In fact, in [19] significant deviations from the simple minded scaling laws are found. This might be taken as an indication for the importance of higher order effects also in the hyperon interactions. In order to overcome the uncertainties remaining in the approach of [19] a DBHF description in the complete SU(3) flavor sector is at present in preparation.

An interesting test case for high density matter are neutron star calculations. Solving the Tolman-Oppenheimer-Volkov (TOV) equation the equation of state of baryonic matter in $\beta-$equilibrium enters as the driving source term. As a result one obtains the mass-radius relation for neutrons stars from which the

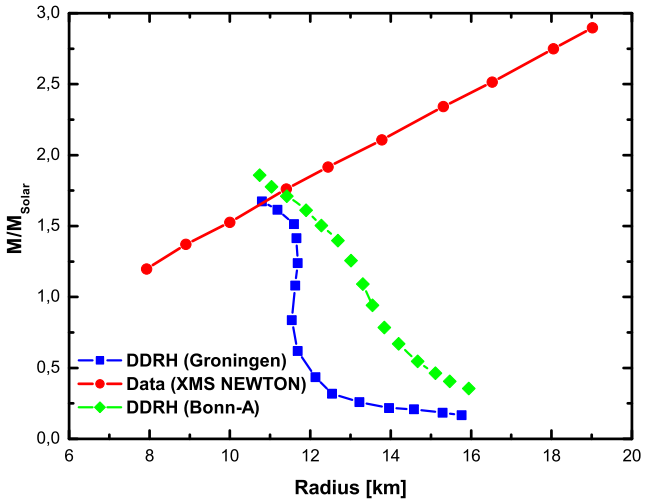


Figure 4: Mass-radius relation (in units of the solar mass) for a neutron star obtained by solving the TOV equations with the DDRH interactions. Results for two free space potentials [9, 18] are compared to the constraint obtained from recent satellite x-ray measurements [21] (full circles).

maximum mass can be read off. Results of such a calculation with the DDRH theory [18] are shown in Fig.4. The DDRH results are compared to recent x-ray measurements [21] for the atomic red-shift $z$ of atmospheric $Fe$ in a neutron star, defining a line $M/M_\odot = zR$ from which, at least, constraints on the allowed mass-radius sector can be derived.

## 4 Spectral Functions in Asymmetric Matter and Fano-Resonances in Dripline Nuclei

Experimentally, increasing evidence is found that the traditional understanding of nuclear structure ceases to be valid when approaching the driplines. This evidence is obtained for a new class of experiments allowing to measure in conjunction with breakup and transfer reactions of exotic nuclei the emission of $\gamma$ rays from the outgoing residual nucleus. Such coincidence measurements show a strong suppression of single particle strength with ground state spectroscopic factors as low as 50% or less. Hence, mean-field dynamics is strongly suppressed in nuclei as e.g. $^{8}$B [29], $^{11}$Li [30], $^{11}$Be [31], $^{17,19}$C [32, 33] and $^{23}$O [34, 35].

Theoretically, this means to go beyond the static mean-field approximation which dominates nuclear binding in stable nuclei. In next order (in the sense of classes of diagrams [9]) the effects of dynamical correlations must be considered. In symmetric nuclear matter and stable nuclei [36, 37, 38, 39] they are known to contribute at a level of only a few percent. In exotic nuclei, however, the correlation self-energies are of the same order or even larger than the binding energies from the static mean-field.

The single particle spectral function [38, 39, 40]

$$a(\omega,p) = \frac{\Gamma(\omega,p)}{(\omega - \frac{p^2}{2m_N} - U(p,k_F) - \mathrm{Re}\Sigma^{ret}(\omega,p,k_F))^2 + \frac{1}{4}\Gamma^2(\omega,p,k_F)} \quad , \tag{7}$$

is defined by the imaginary part of the correlated propagator including the static mean-field potential $U(p,k_F)$ and dispersive contributions from the (retarded) dynamical self-energies $\Sigma^{ret}(\omega,p,k_F)$. The fragmentation of the single particle strength. i.e. the deviation of $a(\omega,p)$ from the mean-field quasi-particle $\delta-$function shape, is described by the width $\Gamma \equiv 2\Im\Sigma^{ret}$. Shifts in energy and momentum are due to the real part of $\Sigma^{ret}$. Spectral functions are an especially sensitive measure for hard processes from short range correlations. As such they are obtaining attention also in the seemingly rather disjoint area of deep inelastic lepton scattering [42] on nuclear targets and hadronic reactions in Compressed Baryonic Matter (CBM) as planned for FAIR@GSI. In the low energy regime – as of interest here – a significant effect is the depletion of hole strength. Results of

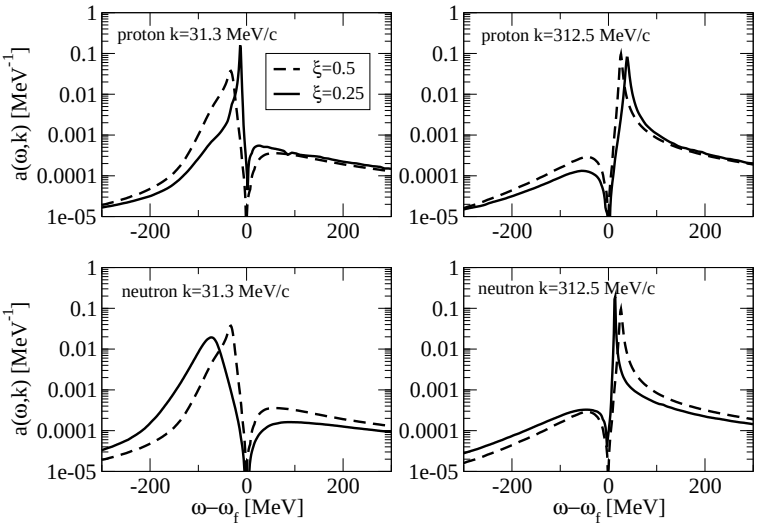


Figure 5: Single particle spectral functions in infinite symmetric ($\xi = Z/A = 0.5$) and asymmetric ($\xi = Z/A = 0.25$) nuclear matter from a transport theoretical calculation [40].

our calculations [40] are shown in Fig.5 where the momentum distributions of infinite asymmetric matter are displayed.

In a finite nucleus dynamical correlations are of a different character. The main difference to infinite matter is that linear momentum is no longer a conserved quantity but instead angular momentum (together with the total energy) becomes a constant of motion. This has important consequences. A clear separation of long- and short range correlations is no longer possible because each nuclear state includes a whole spectrum of momenta. The polarization self-energies are now given by a rather extended sum over angular momenta and integrals over energies [41]. In practice, one needs to include core excitations well beyond the giant resonance region. In Dynamical Core Polarization (DCP) calculations converged results are typically obtained only when states with excitation energies of up to 50 MeV are taken into account. The main contributions are found to come from natural parity excitations, i.e. with parity $\pi_J = (-)^J$, but unnatural parity (magnetic) modes involving spin excitations are not negligible, either.

A prominent DCP feature above the particle emission threshold are Fano resonances [48, 49]. They appear in the low energy continuum close to particle threshold, being created by the interaction of core excited bound states embedded in the continuum *BSEC* with the energetically degenerate elastic single particle background [46]. Spectral functions of this type are displayed in Fig.6. The mean-field part is obtained from a self-consistent microscopic HFB calculation. In the HFB and the QRPA and DCP calculations a non-relativistic G-matrix interaction supplemented by three-body forces was used [45, 47]. The corresponding residual interaction was obtained by Landau-Migdal Fermi liquid theory.

The $^{15}$C$(5/2^+)$ BSEC structures compared in Fig.6 to recent spectroscopic data for $^{15}$C [50] are due the coupling of the $^{14}$C$(0^+, g.s.)$+n d-wave continuum to the $^{14}$C core excited states at $E_C$ = 6.094 $(1^-)$, 6.728 $(3^-)$, 7.012 $(2^+)$, and 8.317 $(2^+)$ MeV. Clearly, such structures will be highly important in the astrophysical capture and knockout reactions contributing to nuclear synthesis in neutron-rich stellar environments.

## 5 Pygmy Dipole Resonances in Exotic Nuclei

A new feature in asymmetric medium and heavy mass nuclei is the appearance of a neutron skin, defined by the difference of the neutron and proton root-mean-square (rms) radii:

$$\delta r = \sqrt{< r^2 >_n} - \sqrt{< r^2 >_p} \quad , \tag{8}$$

Skin nuclei are special because they consist of a core of normal nuclear matter, typically composed of an equal amount of protons and neutrons, and a surface layer of almost pure neutron matter. Hence, part of the neutrons de-mix from the bulk and the question arises under which conditions such systems from particle stable configurations. Theory predicts that different from halo systems skin nuclei are stabilized by shell effects, namely gaining additional binding when a sub-shell is closed or lowered from the continuum into the bound

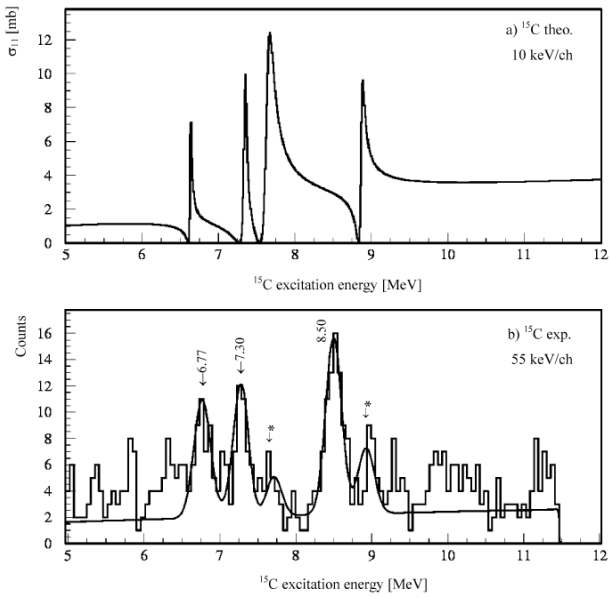


Figure 6: (a) Elastic cross section for the $d_{5/2}$-wave as a function of the $^{15}$C excitation energy.(b) Excitation energy spectrum for the $^{15}$N($^{7}$Li, $^{7}$Be)$^{15}$C reaction at $E_{inc}$ = 55 MeV and $\theta_{lab}$ = 14. Peaks marked with an asterisk correspond to the mutual excitation of 7Be at 0.429 MeV. The continuous line is the sum of the background (the $^{15}$N($^{7}$Li, n$^{7}$Be)$^{14}$C 3-body phase space) and the Gaussians from the fit to the peaks. [46].

state region. However, it is not yet clear whether and how such configurations will affect nuclear properties in general.

An interesting candidate for studying neutron skins are low-lying multipole excitations. A special role is played by low energy dipole excitations close to neutron threshold because they appear only in nuclei with a non-vanishing neutron excess. However, although they are predominantly given by single phonon components the small multi-phonon admixtures are essentially for understanding their energy locations. Also, they have to be distinguished from other known low energy dipole states originating from multiple phonon excitations like the $2^+ \otimes 3^-$ two-phonon states [11, 12]. Theoretically, this requires an extended treatment by taking into account anharmonicities in the excitation spectra from phonon-phonon interactions. A working model is the Quasiparticle Phonon Model (QPM) allowing for anharmonicities from core polarization processes of up to three phonon interactions. In [51] such Pygmy Dipole Resonance (PDR) states have been investigated in the perfectly stable nucleus $^{208}$Pb. As a new aspect the theoretically obtained transition densities and flow pattern of the transition currents were analyzed. Both quantities confirm the genuine character of the PDR states by having a significantly different flow pattern than the GDR states. While the latter are known to be an isovector mode where protons and neutrons oscillate with reverse phases the PDR excitations correspond to the neutron dominated excitation modes with an excess of neutron transition density at the nuclear surface while in the nuclear interior proton excitations are admixed in a phase coherent manner [51].

These observations deserve a more systematic investigation. For that purpose QPM calculations have been performed in the region of the $N = 82$ shell closure. In particular, the low energy excitation spectra in the Sn isotopes have been investigated by QRPA and QPM calculations. An important step was to use single particle energies and wave functions from microscopic HFB calculations. Beside an improved overall description of nuclear ground states the HFB input is essential for extrapolating into the hitherto experimentally unexplored mass regions. Also, varying the neutron number over larger mass ranges should reveal possible correlations between PDR strength and the size of the neutron skin.

Indeed, these expectations were confirmed by the QPM calculations. The PDR states themselves are found to be almost pure QRPA configurations. The full QPM space, however, is required to distinguish properly the PDR and the multi-phonon dipole states. In Fig.7 the PDR strength in the Sn isotopes is compared to the skin thickness. We find a highly interesting correlation between the size of the neutron skin and the PDR strength for $A \gtrsim 112$, increasing almost in parallel. This confirms the signatures of the PDR excitations as a genuine mode of the neutron skin.

However, below $^{110}$Sn and close to $^{100}$Sn, where a proton skin emerges, the situation seems to change. For

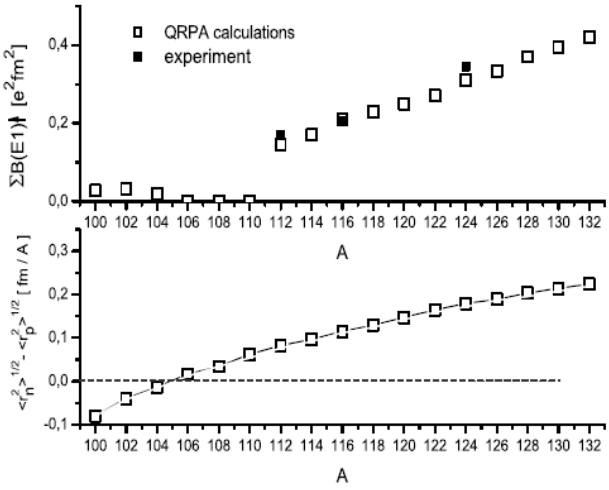


Figure 7: PDR strengths and the mass dependence of the rms-radii in the Sn isotopes are compared.

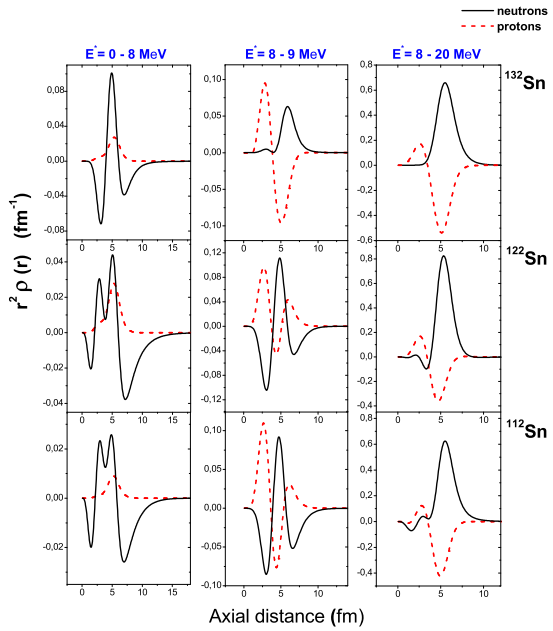


Figure 8: QRPA transition densities of the PDR strength in the Sn isotopes in the PDR energy region (left), the GDR region (middle) and beyond (right).

$A = 100 \cdots 104$ the PDR strength maps nicely the size of the proton skin. For $104 < A < 110$ we encounter a situation where a thin neutron skin exists but the PDR strength remains on a very low level. As recognized in Fig.7 the HFB calculations predict a steady increase of the skin thickness. At $^{112}$Sn a value of about $\delta r \sim 0.06$ fm is reached which seems to be a critical value in the sense that the PDR strength suddenly increases. Looking into the single particle spectra one finds that this is accompanied by a decrease of the energy of the lowest proton-proton 2-QP configuration by about 1 MeV. The PDR response approaches zero around $^{110}$Sn, slightly above the region where the proton and neutron density distributions are balanced. From $^{112}$Sn on, the PDR and the mass dependencies of $\delta r$ are closely correlated. The evolution of the dipole mode from the motion of the neutron skin against the nuclear core in the PDR region to the GDR characteristics of an out-of-phase proton-neutron oscillation mode is seen from the transition densities displayed in Fig.8.

## 6 Summary and Outlook

Nuclear many-body theory was applied to strongly asymmetric nuclear matter and the ground and excited states of dripline nuclei. Interactions were derived from Brueckner and Dirac-Brueckner calculations. In the non-relativistic case by additional density dependencies were supplemented accounting for interaction contributions

beyond the ladder approximation. Dynamical core polarization in neutron-rich nuclei was investigated by HFB and QRPA methods, also accounting for continuum effects. Pygmy dipole modes were investigated in a multi-phonon model. The anharmonicities due to phonon-phonon interactions are important for describing safely the fragmentation pattern and the energy location of the PDR group. The calculations strongly emphasize the importance of continuum coupling, leading to a dissolution of shell structures close to the driplines and Fano resonances above threshold.

The overall features of dripline nuclei are rather well described. However, open and interesting questions remain on the structure of interactions especially in the low-density region. Here, the present treatment of interactions lacks full self-consistency. Especially three-body interactions and induced 2-body interactions from ring diagrams in weakly bound asymmetric nuclear matter and finite nuclei have to be investigated further. Experimentally, this should be complemented by high-resolution measurements of spectral functions in the bound and the continuum region.

## Acknowledgments

This work is supported in part by DFG (contract Le-439), International Graduate School Giessen-Copenhagen-Helsinki-Jyväskylä, GSI Darmstadt and BMBF. Inspiring collaborations with the nuclear structure groups at GSI/FRS and TU Darmstadt are gratefully acknowledged.

## References

[1] C.F. von Weizsäcker, Z. Phys. 96 (1935) 431; H.A. Bethe and R.F. Bacher, Rev. Mod. Phys. 8 (1936) 82.

[2] P.G. Hansen, A.S. Jensen, B. Jonson, *Ann. Rev. Phys. Sci. (N.Y.)* 45 (1995) 591 .

[3] I. Tanihata, Prog.Part.Nucl.Phys. **53** (2004).

[4] G. Münzenberg, Prog.Part.Nucl.Phys. **53** (2004).

[5] H. Lenske, C.M. Keil, Nadia Tsoneva, Prog.Part.Nucl.Phys. **53** (2004) 153.

[6] Proposal for FAIR, Darmstadt, 2004.

[7] F. de Jong, H. Lenske, *Phys. Rev.* C 57 (1998) 3099 .

[8] H. Lenske, F. Fuchs, *Phys. Lett.* B 345 (1995) 355 ; C. Fuchs, H. Lenske, H. Wolter, *Phys. Rev.* C 52 (1995) 3043 .

[9] H. Lenske,Springer Lecture Notes 641 (2004) 147.

[10] R. Machleidt, K. Holinde, C. Elster, *Phys. Rep.* 149 (1987) 1 ; R. Machleidt, *Adv. Nucl. Phys. (N.Y.)* 19 (1989) 189 .

[11] N. Tsoneva, H. Lenske, *Null. Phys.* A 731 (2004) 273 .

[12] N. Tsoneva, H. Lenske, *Phys. Lett.* B 586 (2004) 213 .

[13] N. Tsoneva, H. Lenske, *Phys. Rev.* C (submitted) 2006 .

[14] P. Ring, *et al.*, *Ann. Phys. (N.Y.)* 198 (1990) 132 .

[15] A. Akmal, V. R. Pandharipande, D. G. Ravenhall, *Phys. Rev.* C 58 (1998) 1804 .

[16] E.E. Salpeter, H. A. Bethe, *Phys. Rev.* 84 (1951) 1232 .

[17] F. Hofmann, C. Keil, H. Lenske, *Phys. Rev.* C 64 (2001) 034314 .

[18] F. Hofmann, C. Keil, H. Lenske, *Phys. Rev.* C 64 (2001) 025804 .

[19] C. Keil, F. Hofmann, H. Lenske, *Phys. Rev.* C 61 (2000) 06401 .

[20] C. Keil, H. Lenske, *Phys. Rev.* C 66 (2002) 054307 .

[21] J. Cottam, F. Paerels, M. Mendez, *Nature* 420 (2002) 51 .

[22] G. Audi, A.H. Wapstra, *Null. Phys.* A 595 (1995) 409 .

[23] S. Typel and H.H. Wolter, *Null. Phys.* A 656 (1999) 331 ; S. Typel, T. v. Chossy, and H. H. Wolter, *Phys. Rev.* C 67 (2003) 034002 .

[24] T. Niksic, D. Vretenar, and P. Ring, *Phys. Rev.* C 66 (2002) 064302 ; T. Niksic, D. Vretenar, P. Finelli and P. Ring, *Phys. Rev.* C 66 (2002) 024306 ; T. Niksic, D. Vretenar, and P. Ring, *Phys. Rev.* C 68 (2002) 024310 .

[25] D. Vretenar, A.V. Afanasjev, G.A. Lalazissis, P. Ring, *Phys. Rep.* 409 (2005) 101 .

[26] S. Banik and D. Bandyopadhyay, *Phys. Rev.* C 66 (2002) 065801 .

[27] Guo Hua, Liu Bo, and Zhang Jianwei: *Phys. Rev.* C 67 (2003) 024902 .

[28] H. Lenske, G. Schrieder, *Euro. Phys. J.* A 2 (1998) 41 ; C. Gund, H. Lenske *et al.*, *Euro. Phys. J.* A 10 (2002) 85 .

[29] W. Schwab, H. Geissel, H. Lenske *et al.*, *Z. Phys.* A 350 (1995) 283 ; M.H. Smedberg, H. Lenske *et al.*, *Phys. Lett.* B 452 (1999) 1 ; D. Cortina-Gil, H. Lenske *et al.*, *Phys. Lett.* B 529 (2002) 36 .

[30] M. Zinser, H. Emling, H. Lenske et al., *Null. Phys.* A 619 (1997) 151 .

[31] F. Cappuzzello, H. Lenske *et al.*, *Phys. Lett.* B 516 (2001) 21 .

[32] T. Baumann, H. Lenske *et al.*, *Phys. Lett.* B 439 (1998) 256 .

[33] D. Cortina-Gil *et al.*, *Euro. Phys. J.* A 10 (2001) 49 .

[34] R. Kanungo *et al.*, *Phys. Rev. Lett.* 88 (2002) 142502 .

[35] J. Fernandez, ph.D. Thesis, Univ. Santiago di Compostella, Dec. 2003.

[36] F.J. Eckle *et al.*, *Phys. Rev.* C 39 (1989) 1662 and *Null. Phys.* A 506 (1990) 199 .

[37] F. de Jong, H. Lenske, *Phys. Rev.* C 54 (1996) 1488 .

[38] J. Lehr *et al.*, *Phys. Lett.* B 483 (2000) 324 ;J. Lehr, H. Lenske, S. Leupold, U. Mosel, *Null. Phys.* A 703 (2002) 393 .

[39] F. Froemel, H. Lenske, U. Mosel, *Null. Phys.* A 723 (2003) 544 .

[40] P. Konrad, H. Lenske, U. Mosel, Nucl.Phys. A756 (2005) 192; arXiv preprint nucl-th/0501007.

[41] H. Lenske, C.M. Keil, Nadia Tsoneva, Prog.Part.Nucl.Phys. **53** (2004) 153.

[42] R.F. Sawyer, *Phys. Rev. Lett.* 75 (1995) 2260 .

[43] O. Benhar, A. Fabrocini and S. Fantoni, *Null. Phys.* A 505 (1989) 267 ; O. Benhar, A. Fabrocini and S. Fantoni, *Null. Phys.* A 550 (1992) 201 .

[44] C. Ciofi degli Atti, E. Pace and G. Salme, *Phys. Rev.* C 43 (1991) 1153 .

[45] F. Hofmann, H. Lenske, *Phys. Rev.* C 57 (1998) 183 .

[46] S.E.A. Orrigo, H. Lenske, F. Cappuzzello, A. Cunsolo, A. Foti, A. Lazzaro, C. Nociforo, J.S. Winfield, *Phys. Lett.* B 633 (2006) 469 .

[47] H. Lenske, F. Hofmann, C. Keil, *Prog. Theor. Phys.* 46 (2001) 187 .

[48] U. Fano, Phys. Rev. 124 (1961) 1866.

[49] G. Baur and H. Lenske, *Null. Phys.* A 282 (1977) 201 ; H. Fuchs et al., *Null. Phys.* A 343 (1980) 133 .

[50] F. Cappuzzello, S.E.A. Orrigo, A. Cunsolo, H. Lenske, M.C. Allia, D. Beaumel, S. Fortier, A. Foti, A. Lazzaro, C. Nociforo, S.J. Winfield, Europhys. Lett. 65 (2004) 766.

[51] N. Ryezayeva, H. Lenske *et al.*, *Phys. Rev. Lett.* 89 (2002) 272502 .